

Modeling of X-Ray Emission in Spherical Implosions on OMEGA

Tina Wang

Tina Wang

Modeling of X-Ray Emission in Spherical
Implosions on OMEGA

Tina Wang
Webster Schroeder High School
Rochester, N.Y.

Advisor: Vladimir A. Smalyuk
Research Scientist

Laboratory for Laser Energetics
University of Rochester
Rochester, N.Y.

INTRODUCTION

Our society at present is dependent on fossil fuels. The object of our dependence, however, is a finite resource and the source of both pollution and regional conflict. As a result of the dwindling fossil fuel supply, alternate sources of energy will be needed in the future. While solar, wind, and hydroelectric power are all viable options, each has its own disadvantages. Another possibility, nuclear fission, is considered a dangerous one due to the radioactive nature of the materials used and created in the involved reactions.

There is a cleaner and more ideal way to make energy: nuclear fusion. Fusion does not use a dangerously radioactive fuel source-- instead, the reaction relies on a commonly found element, hydrogen. Unlike the fission reaction, which splits a heavy, radioactive atom, fusion combines two smaller atoms into a larger one; both processes follow the concept of converting mass into energy. As the materials involved in fusion are much less dangerous and practically inexhaustible as a resource, the advent of a reactor capable of maintaining the reaction to produce power for human needs is highly desirable.

The Laboratory for Laser Energetics (LLE) at the University of Rochester, with its 60 -beam OMEGA laser system, is a leading institution in direct-drive inertial confinement fusion (ICF). Laser-induced ICF at LLE involves the irradiation of a target capsule about 1 mm in diameter, usually containing the hydrogen isotopes deuterium and tritium. The laser beams cause the target to heat up to extreme temperatures. The outer shell of the target explodes outward, causing the inner portion of the target to implode, dramatically compressing the target and increasing its density so fusion can occur.

OMEGA currently uses D_2 as fuel for its target pellets because D_2 targets are easier to produce than DT targets and are more useful for

diagnosing the target's conditions near peak compression. Primary fusion reactions with D_2 can occur in two ways. Deuterium can react with deuterium to produce a Helium isotope with ~~three~~^{one} neutron~~s~~ and a free neutron: $D + D \rightarrow {}^3\text{He} (0.82 \text{ MeV}) + n (2.45 \text{ MeV})$. Deuterium can also react with deuterium to produce a tritium atom and a proton: $D + D \rightarrow T (1.01 \text{ MeV}) + p (3.02 \text{ MeV})$. Each of these reactions has an equal probability of occurring, and each primary reaction results in products that can also undergo fusion: $D + T (0 \text{ to } 1.01 \text{ MeV}) \rightarrow {}^4\text{He} + n (11.9 \text{ to } 17.2 \text{ MeV})$. The ability for both primary and secondary reactions to occur with maximum yield depends on the temperature and density of the imploded target.

If the target is not irradiated uniformly, it can be subject to irregularities due to Raleigh-Taylor instability and will not implode uniformly. These irregularities cause the plastic shell and fuel to mix and prevent the target from reaching high enough temperature and density for the above reactions to continue at maximum efficiency. The perturbations that result cause the fusion reaction to lose its dynamic. They therefore stand as another obstacle to the attainment of ignition. The deviations caused by Raleigh-Taylor instability can be seen through images mapping the intensity of x-rays emitted by the target during the experiments. Therefore, it is important to consider images of x-ray emission while trying to diagnose what conditions the target was subject to during irradiation and implosion and how these conditions deviated from those in an "ideal" experiment. The project described in this report involved using computer programs written in the PV-Wave language to calculate and visualize x-ray intensity using both experimental and theoretical data, then attempted to find density and charge profiles that would generate x-ray intensity images similar to ones captured experimentally.

METHODS

Experimental Configuration

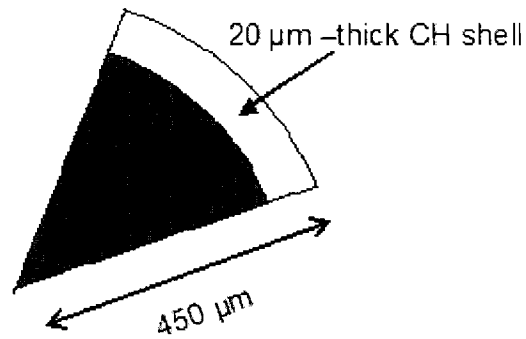


Figure 1. Diagram of deuterium-filled plastic pellet.

The experiment was carried out with a target sphere with an initial radius of approximately 450 μm . This target consisted of a plastic CH shell, about 20 μm thick, filled with 15 atm deuterium gas (fig. 1). The target was driven by 60, 351 nm laser beams by the OMEGA system, inputting energy of a total of ~ 23 kJ in a 1-ns, square-shaped pulse.

Data Collection

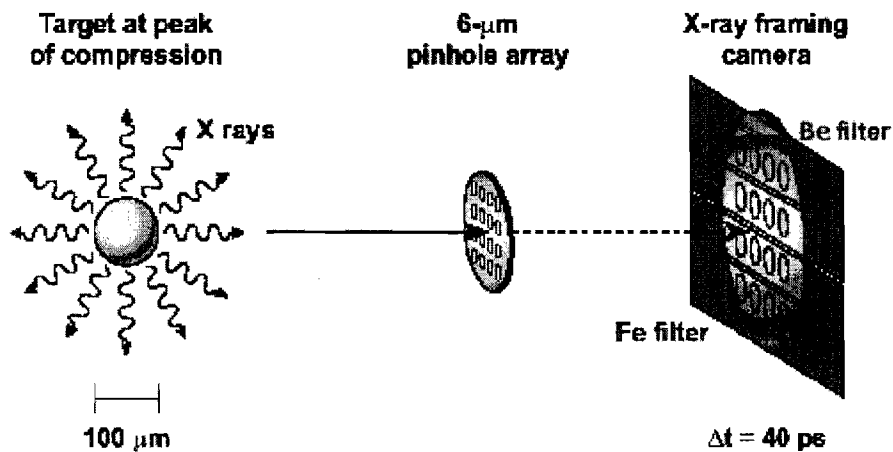


Figure 2. Capturing images of x-ray intensity.

Images mapping x-ray intensity were captured by an x-ray framing camera (fig. 2). X-rays were emitted by the target during peak compression;

these x-rays first encountered a 6 μm pinhole array, then a 200 μm Be filter and a 50 μm Fe filter. Only photons of a certain energy could pass through these filters and proceed. These selected photons then met a microchannel plate (MCP), followed by a phosphor plate. The X-ray photons struck the pores of the MCP, ejecting electrons via the photoelectric effect, which were multiplied in number as they struck the sides of the pores, ejecting even more electrons from the material of the pores. The electrons then hit the phosphor plate, ionizing it and producing an image representing the x-ray intensity of the target at a given time as the target nears peak compression. The camera was designed to capture a series of progressive images at $\sim 40\text{ps}$ time intervals by running a voltage pulse along the MCP.

ANALYTICAL TECHNIQUES USED

Simulation Under Ideal Conditions

$$\frac{dI_v}{ds} = \frac{\mathcal{E}}{4\pi} - kI_v$$

$$\mathcal{E} = 3.031024 \times 10^{-15} z^2 d^2 e^{\frac{-\text{energy}}{T}}$$

The free-free absorption and emission radiation transport equation solves for x-ray intensity, I_v (in au) in relation to distance (s , in microns) from the center of the target. The Emissivity is \mathcal{E} , k is the absorption coefficient, and z is the charge of the target, d the target's density (cm^{-3}), and T its temperature (eV). Energy is measured in units of eV. Theoretical data simulating the temperature, density, and charge of the target had it reached peak compression under ideal conditions were provided. The data profiles' information was placed into a two-dimensional, 400 by 400 array, each point in the array representing a value for temperature, density, charge, and ionic temperature, since solving for x-ray intensity by integration required data to be in two dimensions. Taken as a whole, these arrays represented images of

the above properties' respective values with respect to distance from the center of the target, in microns (fig. 3).

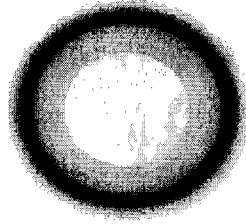


Figure 3. Array of ideal data modeling electron temperature.

The program integrated each of these data arrays (of electron temperature, density, and charge) down their columns (defined as each one-pixel vertical line down the array) to solve the equation for x-ray intensity, producing a one-dimensional array of values that essentially represented x-ray intensity as a function of radius (distance in microns from the center of the image).

Another program took the above lineout of intensity and produced a two-dimensional representation of the x-ray intensity image (similar to the profiles that had been used to generate the x-ray lineout) by setting the value at a certain index in the one-dimensional array at every point in a two-dimensional array that distance away from the center of the image. This was possible because the data was ideal and the produced image had radial symmetry. Each of these intensity images was 400 pixels in width, simulating a circular area modeling the center of the target. These circular models' diameters varied, becoming very small as the target reach peak compression. The images were then run through a series of calculations that simulated the effects that the numerous filters would have on x-ray intensity. These included a 200 μm Be filter, a 50 μm Fe filter, and a resolution filter that was applied through the Fast Fourier Transform (FFT) function on PV-Wave. The Be and Fe filter simulations acted as their experimental equivalents would have, allowing only photons of a certain energy to pass

through them, while the resolution filter moderated the sharp peaks in the original intensity lineout to reduce noise by spreading the intensity at each pixel in the original image over an area with the shape given by the graph (fig. 4).

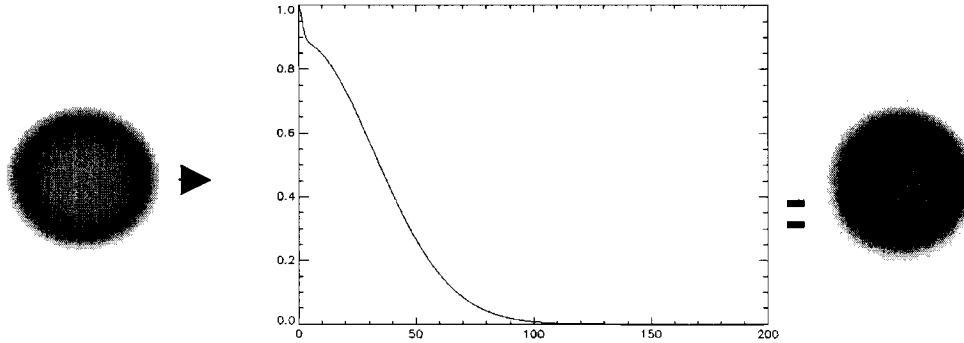


Figure 4. Modulation Transfer Function.

Simulating Modulations

Density and charge profiles were generated in a trial-and-error attempt to produce lineouts of intensity similar to those of the experiments. Different density and charge profiles were characterized by relative areal-density nonuniformity. Instead of the perfectly symmetrical data that had been used to generate ideal x-ray images, irregularities were now imposed upon the density and charge profiles in order to create a less-symmetric and more realistic representation of the imploding plastic pellet. Profiles with modulations were created by polar functions generating irregular, non-symmetric graphs about the origin. By altering the amplitude or constant term of the polar function, the areal-density nonuniformity could be modified and the profile could be made to have more or less wave-like modulations. These profiles were then run through the program for calculating x-ray intensity and used to create lineouts to compare with experimental ones.

RESULTS/DISCUSSIONS

Comparison of Experimental Images with Ideal Images

The intensity images produced with ideal profiles of density, charge, and temperature agreed fairly well with the experimental data (fig. 5). However, the experimental images showed intensity near the center of the image and the generated, ideal intensity images displayed a bright-ring characteristic, indicating that the intensity peaked around the circumference of the circular image. The only explanation for this deviance was that the experimental target had imploded nonuniformly, resulting in modulations that produced the center peak of x-ray intensity.

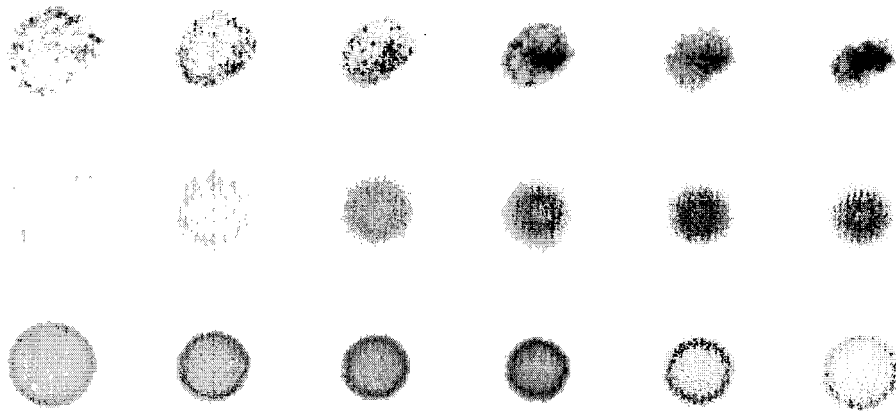


Figure 5. Comparison of experimental images (top row) with images from LILAC (middle row) and nonuniformly generated images (third row).

Profiles were simulated using polar graphs of trigonometric functions, in the form of $r(\theta) = \sin(a_1\theta + c_1) + \cos(a_2\theta + c_2) + \dots$, where a_1, a_2, c_1, c_2 , and so on are constants. It was found that, if the simulated profile had too large of an areal-density nonuniformity, it would generate a lineout with too many wavelengths (fig. 6).

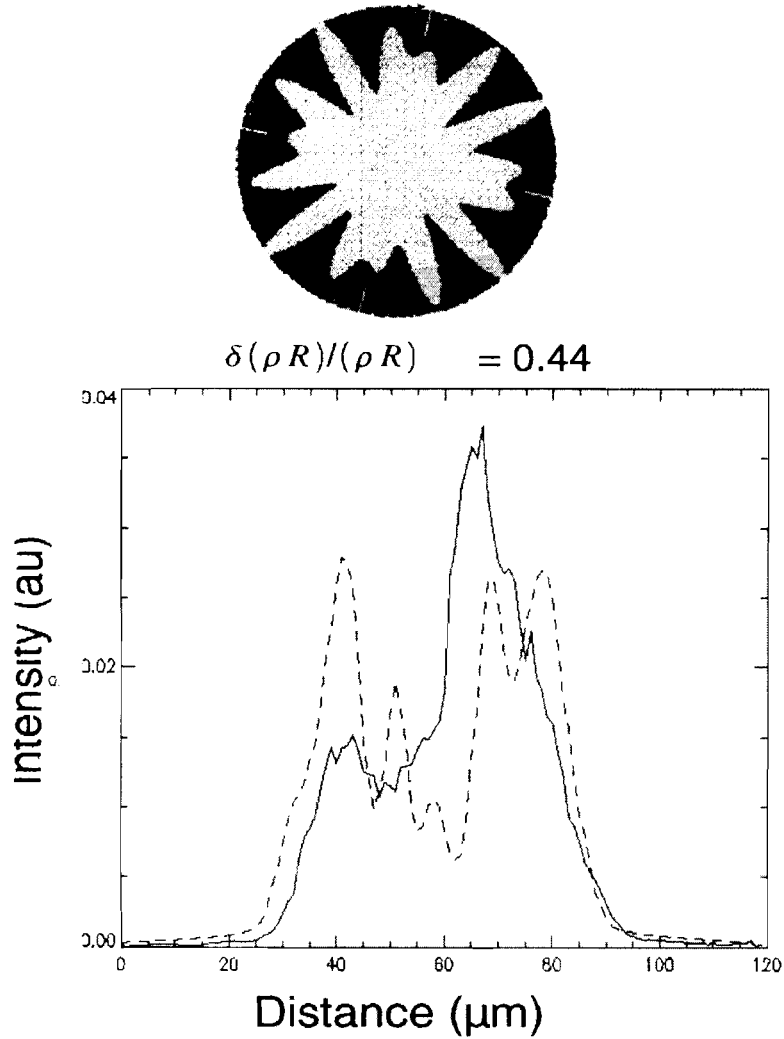


Figure 6. Comparison of generated (dotted line) and experimental lineout (solid line).

Conversely, if the profile had little or no areal-density nonuniformity, it would generate a lineout with too few wavelengths. It was found that profiles with about 18% areal-density nonuniformity produced x-ray intensity lineouts that resembled the experimental data the closest (fig. 7)

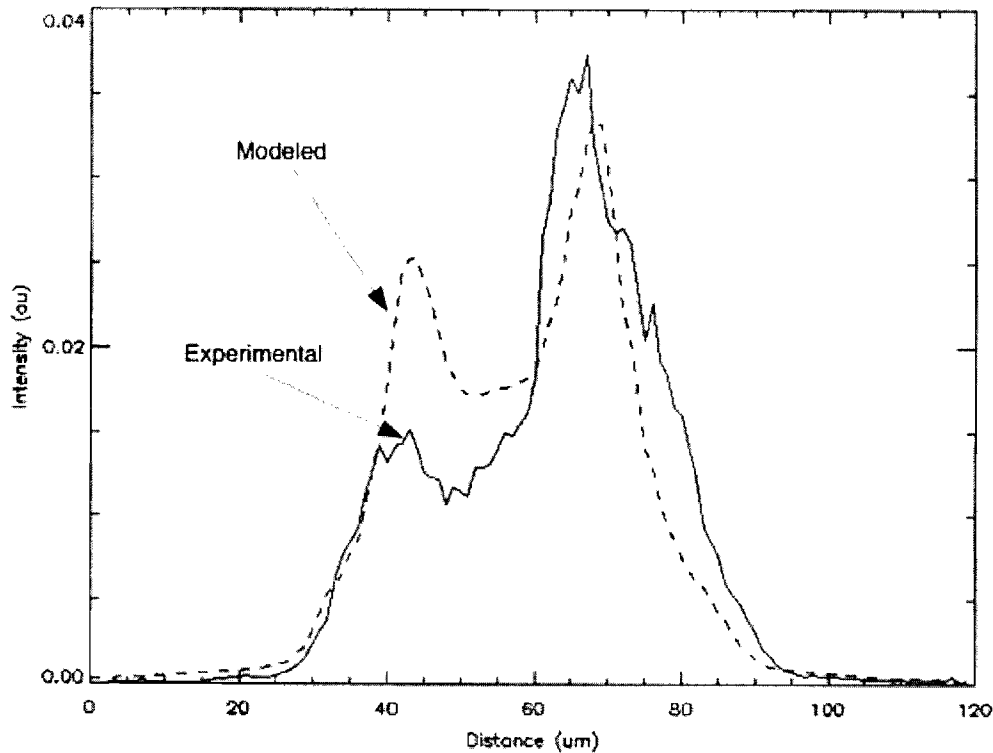


Figure 7. Best comparison of generated (dotted line) and experimental lineout (solid line).

CONCLUSIONS

Using simulated profiles of imploding targets, x-ray intensity lineouts of such targets were generated and compared with experimental data to determine the experimental conditions of the reaction. X-ray lineouts of targets that had undergone idealized implosion were also produced; the experimental lineouts were then compared with the theoretical and found to be in good agreement, but they were not entirely similar. It was decided that the dissimilarities were a result of modulations present in the experimental profiles. Thus, modulations were imposed on simulated profiles to better mimic experimental lineouts (in the future, a method different from the trial-and-error approach used for modeling described in this report might be more desirable). It was found that increasing the areal-density nonuniformity of a

profile increased the number of wavelengths present on the generated x-ray lineout. After determining that too large of an areal-density nonuniformity produced an x-ray lineout with too many wavelengths and little or no areal-density nonuniformity generated too symmetrical and ideal of a lineout, it was found that lineouts generated by profiles with 18% areal-density nonuniformity agreed with the best experimental lineouts.

ACKNOWLEDGEMENTS

Thanks are given to Dr. Vladimir Smalyuk, whose guidance made this project possible.